Topics in Mathematical Physics, General Relativity and Cosmology in Honor of Jerzy Plebański

Proceedings of 2002 International Conference

Cinvestav, Mexico City 17 – 20 September 2002

Editors

Hugo García-Compeán

Bogdan Mielnik

Merced Montesinos

Maciej Przanowski

World Scientific

NEW JERSEY • LONDON • SINGAPORE • BEIJING • SHANGHAI • HONG KONG • TAIPEI • CHENNAI

STRUCTURE FORMATION IN THE LEMAîTRE-TOLMAN COSMOLOGICAL MODEL (A NON-PERTURBATIVE APPROACH)

ANDRZEJ KRASIŃSKI*

N. Copernicus Astronomical Centre, Polish Academy of Sciences,
Bartycka 18, 00 716 Warszawa, Poland
Email: akr@camk.edu.pl

CHARLES HELLABY

Department of Mathematics and Applied Mathematics,
University of Cape Town
Rondebosch 7701, South Africa
Email: cwh@maths.uct.ac.za

Structure formation is described by a Lemaître-Tolman model such that the initial density perturbation within a homogeneous background has a smaller mass than the structure into which it will develop, and accretes more mass during evolution. It is proved that any two spherically symmetric density profiles specified on any two constant time slices can be joined by a Lemaître-Tolman evolution, and exact implicit formulae for the arbitrary functions that determine the resulting L-T model are obtained. Examples of the process are investigated numerically.

1 The problem

Attempts to describe the structure formation in the Universe are dominated by the perturbative approach. In this approach, one assumes that proto-galaxies, or proto-clusters of galaxies appeared as small-amplitude condensations in a homogeneous background (caused by means poorly understood, although much speculated about), and were later enhanced by "gravitational instability". This means, additional matter was captured onto these initial condensations by their gravitational attraction. The basic weakness of this approach is that the evolution of the condensations cannot be followed to the present time because the current density amplitude is no longer small.

This calls for the use of exact solutions of Einstein's equations. Here, we shall use the Lemaître-Tolman[1,2] (L-T) model. Its weaknesses are: 1. Spherical symmetry – which does not allow to include rotation in the description, and 2. Dust source – which excludes thermo/hydrodynamics in the early stages of evolution. In spite of this, the model can describe the formation of a galaxy cluster with remarkable accuracy.

The very existence of inhomogeneous cosmological models shows that non-Friedmannian distributions of density and velocity would have been coded in the Big Bang and need not be "explained" as fluctuations that appeared within a homogeneous background during evolution. Moreover, since the L-T collection of models is labelled by two arbitrary functions of mass, that reduce to specific forms in the Friedmann limit, it follows that the Friedmann models are very improbable statistically. Assuming that our physical Universe is homogeneous indeed, one needs to explain how homogeneity might have come about out of inhomogeneous

*THIS RESEARCH WAS SUPPORTED BY THE POLISH RESEARCH COMMITTEE GRANT NO 2 P03B 060 17 AND BY A GRANT FROM THE SOUTH AFRICAN NATIONAL RESEARCH FOUNDATION

initial data, not the other way round. However, in this paper we have accepted a high degree of homogeneity at decoupling, and we determined that a sufficiently rapid growth of condensations to change them into a galaxy cluster by today is possible.

The detailed calculations, although based on exact formulae, had to be carried out numerically.

This report is an abridged version of the published paper Ref. 3.

2 Basic properties of the Lemaître-Tolman model.

The Lemaître-Tolman (L-T) model[1,2,4] is a spherically symmetric nonstatic solution of the Einstein equations with a dust source. Its metric is:

$$\mathrm{d}s^2 = \mathrm{d}t^2 - \frac{{R_{,r}}^2}{1+2E(r)}\mathrm{d}r^2 - R^2(t,r)(\mathrm{d}\vartheta^2 + \sin^2\vartheta \mathrm{d}\varphi^2), \tag{2.1}$$

where $E(r)$ is an arbitrary function, $R_{,r} = \partial R(t,r)/\partial r$, and R obeys

$${R_{,t}}^2 = 2E(r) + 2M(r)/R + \frac{1}{3}\Lambda R^2, \tag{2.2}$$

where Λ is the cosmological constant. Eq. (2.2) is a first integral of one of the Einstein equations, and $M(r)$ is another arbitrary function. The matter-density is:

$$\kappa\rho = \frac{2M_{,r}}{R^2 R_{,r}}, \qquad \text{where } \kappa = \frac{8\pi G}{c^4}. \tag{2.3}$$

In the following, we will assume $\Lambda = 0$. Then the solutions of eq. (2.2) are:
When $E < 0$:

$$R(t,r) = -\frac{M}{2E}(1-\cos\eta),$$

$$\eta - \sin\eta = \frac{(-2E)^{3/2}}{M}(t - t_B(r)). \tag{2.4}$$

where η is a parameter; when $E = 0$:

$$R(t,r) = \left[\frac{9}{2}M(t-t_B(r))^2\right]^{1/3}, \tag{2.5}$$

and when $E > 0$:

$$R(t,r) = \frac{M}{2E}(\cosh\eta - 1),$$

$$\sinh\eta - \eta = \frac{(2E)^{(3/2)}}{M}(t - t_B(r)), \tag{2.6}$$

where $t_B(r)$ is one more arbitrary function (the bang time). Note that eqs. (2.1) – (2.6) are covariant under arbitrary coordinate transformations $r = g(r')$. This means one of the functions $E(r)$, $M(r)$ and $t_B(r)$ can be fixed at our convenience by a choice of g.

The Friedmann models are contained in the Lemaître-Tolman class as the limit:

$$t_B = \text{const}, \qquad |E|^{3/2}/M = \text{const}, \tag{2.7}$$

and one of the standard radial coordinates for the Friedmann model results if, in addition, the coordinates in (2.4) – (2.6) are chosen so that $M = M_0 r^3$, where M_0 is an arbitrary constant; then it follows that $E/r^2 = \text{const} := -k/2$.

It will be convenient to use $M(r)$ as the radial coordinate (i.e. $r' = M(r)$). This is possible because in the structure formation context one does not expect any "necks" or "bellies" where $M_{,r} = 0$, so $M(r)$ should be a strictly increasing function in the whole region under consideration. Then:

$$\kappa\rho = 2/(R^2 R_{,M}) \equiv 6/(R^3)_{,M}\,. \tag{2.8}$$

We will also assume that there are no shell crossings[5] because the L-T co-moving description breaks down there.

3 The evolution as a mapping from an initial density to a final density.

The evolution of the L-T model is usually specified by defining initial conditions, e.g. the density $\rho(t_1, R)$ and velocity $R_{,t}(t_1, R)$ at an initial instant $t = t_1$. In this approach, one tries to "shoot" into the desired final state. It is, however, possible, to approach the problem in a different way: to specify the density distributions at two different instants, $t = t_1$ and $t = t_2$, calculate the corresponding $E(M)$ and $t_B(M)$, and in this way obtain a definite model. It will be proven below that any initial value of density at a specific position ($r, M = \text{const}$) can be connected to any final value of density at the same position by one of the Lemaître-Tolman evolutions (either $E > 0$, or $E < 0$, or, in an exceptional case, $E = 0$). In the Friedmann limit, any two constant densities can be connected by one of the $k > 0$, $k < 0$ or $k = 0$ Friedmann evolutions. (The shell crossings have to be checked for after the model is constructed.)

It will be assumed that $t_2 > t_1$, and that the final density $\rho(t_2, M)$ is smaller than the initial density $\rho(t_1, M)$ at the same M, for each M. This means that matter has expanded along every world-line, but the proof can be adapted to the collapse situation.

3.1 Hyperbolic regions

Let us consider the L-T model with $E > 0$. Let the initial and final density distributions at $t = t_1$ and $t = t_2$ be given by:

$$\rho(t_1, M) = \rho_1(M), \qquad \rho(t_2, M) = \rho_2(M). \tag{3.1}$$

From (2.3) we then have, for each of t_1 & t_2:

$$R^3(t_i, M) - R^3_{\min i} = \int_{M_{\min}}^{M} \frac{6}{\kappa\rho_i(M')}\,\mathrm{d}M' := {R_i}^3(M), \qquad i = 1, 2 \tag{3.2}$$

and $R_2(M) > R_1(M)$ in consequence of $\rho(t_2, M) < \rho(t_1, M)$. We will assume there is an origin where $M = 0$ and $R(t_i, 0) = 0$, so that $R_{\min i} = 0 = M_{\min}$ is valid. Solving (2.6) for $t(R, r)$ and writing it out for each of (t_1, R_1) and (t_2, R_2) leads to:

$$t_B = t_i - \frac{M}{(2E)^{3/2}}\left[\sqrt{(1 + 2ER_i/M)^2 - 1} - \operatorname{arcosh}(1 + 2ER_i/M)\right], \qquad i = 1, 2, \tag{3.3}$$

and then eliminating t_B between the two versions of (3.3) we find:

$$\sqrt{(1 + 2ER_2/M)^2 - 1} - \operatorname{arcosh}(1 + 2ER_2/M)$$
$$-\sqrt{(1 + 2ER_1/M)^2 - 1} + \operatorname{arcosh}(1 + 2ER_1/M) = [(2E)^{3/2}/M](t_2 - t_1). \tag{3.4}$$

For ease of calculations, let us denote:

$$x := 2E/M^{2/3}, \qquad a_i = R_i/M^{1/3}, \quad i = 1, 2;$$

$$\psi_H(x) := \sqrt{(1+a_2x)^2-1} - \operatorname{arcosh}(1+a_2x) - \sqrt{(1+a_1x)^2-1} + \operatorname{arcosh}(1+a_1x)$$

$$-(t_2-t_1)x^{3/2}. \tag{3.5}$$

Our problem is then equivalent to the following question: for what values of the parameters $a_2 > a_1$ and $t_2 > t_1$, does the equation $\psi_H(x) = 0$ have a solution $x \neq 0$?

By an elementary analysis of the properties of the function $\psi_H(x)$, it can be verified that $\psi_H(x) = 0$ has a positive solution if and only if

$$t_2 - t_1 < \frac{\sqrt{2}}{3}\left({a_2}^{3/2} - {a_1}^{3/2}\right), \tag{3.6}$$

and that the solution is unique (see Ref. 3). Hence, this is a necessary and sufficient condition for the existence of an $E > 0$ evolution connecting $R(t_1, M)$ to $R(t_2, M)$. Eq. (3.6) is equivalent to the statement that between t_1 and t_2, $R(t, M)$ increased by more than it would have increased in the $E = 0$ L-T model.

For the numerical calculation of $E(M)$ it is useful to know that the $x_H > 0$ for which $\psi_H(x_H) = 0$ obeys $x_H < x_A$, where

$$x_A = \frac{(a_2-a_1)^2}{(t_2-t_1)^2} \tag{3.7}$$

(see Ref. 3 again).

3.2 Still-expanding elliptic regions

For $E < 0$, a similar result holds, but with one refinement: depending on the value of $(t_2 - t_1)$, the final density will be either in the expansion phase or in the recollapse phase.

If the final density is still in the expansion phase, then $\eta \in [0, \pi]$ for both values of t. The analogs of eqs. (3.3) and (3.4) are then:

$$t_B = t_i - \frac{M}{(-2E)^{3/2}}\left[\arccos(1+2ER_i/M) - \sqrt{1-(1+2ER_i/M)^2}\right], \tag{3.8}$$

$$\psi_X(x) = 0, \tag{3.9}$$

where this time

$$x := -2E/M^{2/3},$$

$$\psi_X(x) := \arccos(1-a_2x) - \sqrt{1-(1-a_2x)^2} - \arccos(1-a_1x) + \sqrt{1-(1-a_1x)^2}$$

$$-(t_2-t_1)x^{3/2}, \tag{3.10}$$

the definitions of a_i being still (3.5).

This time the arguments of arccos must have absolute values not greater than 1. This implies $x \leq 2/a_i$ for both i, and so, since $a_2 > a_1$

$$0 \leq x \leq 2/a_2, \tag{3.11}$$

which means: if there is any solution of (3.9), then it will have the property (3.11). The two square roots in (3.10) will then also exist. Eq. (3.11) is equivalent to the requirement that $(R_{,t})^2$ (in (2.2) with $\Lambda = 0$) is nonnegative at both t_1 and t_2.

Here, the necessary and sufficient condition for the existence of a positive solution of $\psi_X(x) = 0$ is the set of two inequalities

$$\frac{\sqrt{2}}{3}\left({a_2}^{3/2} - {a_1}^{3/2}\right) < t_2 - t_1$$

$$\leq (a_2/2)^{3/2}\left[\pi - \arccos(1 - 2a_1/a_2) + 2\sqrt{a_1/a_2 - (a_1/a_2)^2}\right]. \tag{3.12}$$

The first inequality means that the model must have expanded between t_1 and t_2 by less than the $E = 0$ model would have done. The second one just re-expresses the fact that t_2 is not later than the maximal expansion stage (see Ref. 3 for details).

3.3 Recollapsing elliptic regions

The reasoning above applied only in the increasing branch of R in (2.4). For the decreasing branch, where $\eta \in [\pi, 2\pi]$, instead of (3.9) – (3.10) we obtain

$$\begin{aligned} t_B &= t_1 - \frac{M}{(-2E)^{3/2}}\left[\arccos(1 + 2ER_1/M) - \sqrt{1 - (1 + 2ER_1/M)^2}\,\right] \\ &= t_2 - \frac{M}{(-2E)^{3/2}}\left[\pi + \arccos(-1 - 2ER_2/M) + \sqrt{1 - (1 + 2ER_2/M)^2}\,\right] \end{aligned} \tag{3.13}$$

and

$$\psi_C = 0, \qquad \text{where}$$

$$\psi_C(x) := \pi + \arccos(-1 + a_2x) + \sqrt{1 - (1 - a_2x)^2} - \arccos(1 - a_1x) + \sqrt{1 - (1 - a_1x)^2}$$

$$-(t_2 - t_1)x^{3/2}. \tag{3.14}$$

The necessary and sufficient condition for the existence of an $x > 0$ obeying $\psi_C(x) = 0$ is

$$t_2 - t_1 \geq (a_2/2)^{3/2}\left[\pi - \arccos(1 - 2a_1/a_2) + 2\sqrt{a_1/a_2 - (a_1/a_2)^2}\right]. \tag{3.15}$$

3.4 General remarks

The above analysis considered only single world-lines, that is, single M values. We extend this to the whole of $\rho_i(M)$ by noting that $E(M)$ and $t_B(M)$ are arbitrary functions in the L-T model, and so continuous ρ_i will generate continuous E & t_B.

In (3.6), at M values where $t_2 - t_1 = (\sqrt{2}/3)({a_2}^{3/2} - {a_1}^{3/2})$, the final state results from the initial one by a parabolic ($E = 0$) evolution. In (3.12) and (3.15), for M values where the equality holds, the final state is at the local moment of maximal expansion.

When $E < 0$, the signature of the metric requires that

$$E(M) \geq -1/2, \tag{3.16}$$

and so, once $E(M)$ has been calculated, (3.16) will have to be checked. Note that the $k < 0$ Friedmann model in standard coordinates has this problem, too — with $2E = -kr^2$, blindly continuing through $r = 1/\sqrt{k}$ will make $E < -1/2$ and $M > M_{Universe}$.

The shell crossings, where the density diverges and changes sign, may occur, and so the conditions on $E(M)$ & $t_B(M)$ for avoiding them[5] must also be checked. However, if they occur before t_1 or after t_2, this may not be of much concern.

Our result can be stated as the

Theorem Given any two times t_1 and $t_2 > t_1$, and any two spherically symmetric density profiles $0 < \rho_2(M) < \rho_1(M)$ defined over the same range of M, a L-T model can be found that evolves from ρ_1 to ρ_2 in time $t_2 - t_1$. The inequalities (3.6)/(3.12)/(3.15) will tell which class of L-T evolution applies at each M value. The possibilities of shell crossings or excessively negative energies must be separately checked for.

Note that the individual values of t_1 and t_2 have no physical meaning. It is the difference $(t_2 - t_1)$ that, together with ρ_1 and ρ_2, determines a L-T model, i.e. determines the functions $E(M)$ and $t_B(M)$. The "age of the Universe" (which is a *local* quantity in the L-T models) at the initial and final instant is then calculated as $(t_1 - t_B)$ and $(t_2 - t_B)$, respectively.

4 Implications for the Friedmann models.

These considerations apply to the Friedmann limit, provided one retains the curvature index k as an arbitrary constant. If one starts out with the curvature index already scaled to $+1$ or -1 when it is nonzero, unexpected difficulties appear. For example, the Friedmann limit of the inequality (3.6) does not appear at all, and one gets the false illusion that each pair of (t_i, ρ_i) states can be connected by a $k > 0$ Friedmann evolution. The remaining part of this section is meant to explain the source of this difficulty.

The quantity $x = \pm 2E/M^{2/3}$ that was being determined in sec. 3 by the assumed density distributions, becomes $\mp k/{M_0}^{2/3}$ in the Friedmann limit, where $M_0 = (4/3)\pi(G/c^2)\times \rho(t)S^3(t)$ is the Friedmann mass integral. With $k < 0$, it is k that determines the model, and M_0 only characterizes the sub-volume of the model that we follow. To see this, recall the law of evolution of S that results from (2.2) in the limit given by $\Lambda = 0$ and (2.7):

$$ {S_{,t}}^2 = -k + 2M_0/S. \tag{4.17} $$

When $k < 0$, the lifetime of the model is infinite, and different models differ by the asymptotic velocity of expansion, $\lim_{S\to\infty} S_{,t} = \sqrt{-k}$ – which is independent of M_0. When $k > 0$, both k and M_0 determine the model (M_0 is proportional to the mass of the Universe, and k is a measure of the total energy – gravitational potential energy + the kinetic energy of expansion). When $k = 0$, M_0 can be scaled to any value by coordinate transformations.

Now let us see what happens when $k \neq 0$ is scaled to ± 1 by coordinate transformations. Fig. 1 shows the evolution of Friedmann models with different values of k. The metric is:

$$ \mathrm{d}s^2 = \mathrm{d}t^2 - S^2(t)\left[\frac{\mathrm{d}r^2}{1-kr^2} + r^2\left(\mathrm{d}\vartheta^2 + \sin^2\vartheta \mathrm{d}\varphi^2\right)\right]. \tag{4.18} $$

In order to achieve $k = \pm 1$, we transform:

$$ r = r'/\sqrt{|k|}, \qquad \bar{S} = S/\sqrt{|k|}. \tag{4.19} $$

In the limit $k \to 0$, $\bar{S} \to \infty$ at all values of t, i.e. the $k = 0$ graph in Fig. 1 becomes the vertical straight half-line $\{t = t_0, S \geq 0\}$, the part of Fig. 1 that was above that graph disappears – and the illusion arises that any two points in the quarter-plane $\{t > t_0, S > 0\}$ can be connected by a $k > 0$ evolution. If the rescaling $|k| \to 1$ is done first, taking the limit $k \to 0$ within the Friedmann family becomes impossible, and the Friedmann limits of the inequalities (3.6) and (3.12) do not come up.

Now, comparing different Friedmann models and choosing the one that best fits the observational constraints is what observational cosmology is mostly about. However, astronomers use the models with k already scaled to ± 1...

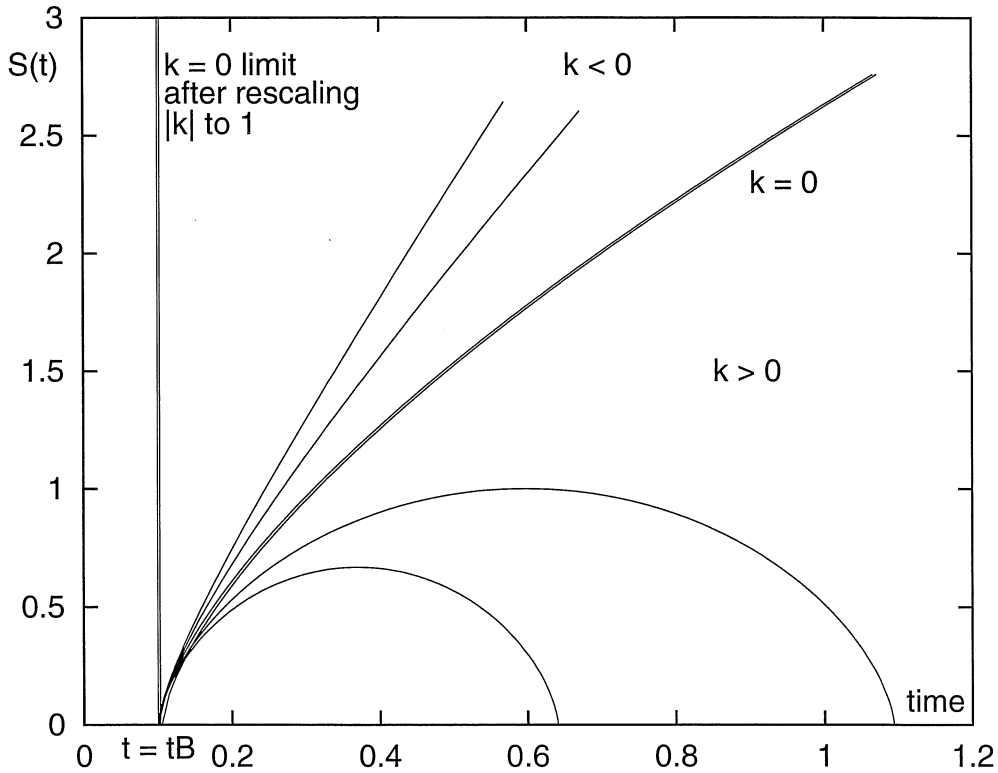

Figure 1. The functions $S(t)$ corresponding to Friedmann models with different values of k. When $k \to 0$, the rescaling of S required to achieve $|k| = 1$ maps the $k = 0$ graph into the vertical straight line at $t = t_0$, and no place is left for the $k < 0$ models.

5 Numerical Example

5.1 Past null cones, horizons and scales on the CMB sky

The age of the universe is currently believed to be about 14 Gyr. In a $k = 0$ dust (Friedmann) model, $H_0 = 65$ km/s/Mpc implies $t_0 = 2/3H_0 = 10$ Gyr, which puts t_r at 10^5 yr. We shall assume this Friedmann model (with $\Lambda = 0$) as the background.

The physical radius of the past null cone in a $k = 0$ Friedmann model ($S \propto t^{2/3}$) is

$$L(t) = S \int_t^{t_0} \frac{1}{S}\, dt = 3c\,(t_0^{1/3} t^{2/3} - t), \tag{5.1}$$

so an observed angular scale of θ on the CMB sky has a physical size at recombination of

$$L_r = L(t)\,\theta = 3c\,(t_0^{1/3} t_r^{2/3} - t_r)\,\theta. \tag{5.2}$$

The present day size of the observed structure — assuming it doesn't collapse — is merely scaled up by the ratio of scale factors

$$L_0 = L_r \frac{S_0}{S_r}. \tag{5.3}$$

The condensed structures (stars, galaxies, clusters of galaxies, etc) that exist today had not yet existed at the recombination time. To determine the angle that they would subtend on the CMB sky, we calculate the radius that the matter of a given object would fill if it were

diluted to the present background density; it is

$$L_{c0} = \left(\frac{3M_c}{4\pi\rho_{b,0}} \right)^{1/3} , \tag{5.4}$$

and then the corresponding size L_{cr} at t_r is calculated from (5.3).

5.2 Scales in the perturbation

We imagine that present day structures accreted their mass from a background that was close to Friedmannian, and therefore the scale of the matter that is destined to end up in a present day condensation is fixed by its present day mass.

The COBE data shows $\delta T/T \sim 10^{-5}$ on scales of 10°, and the density perturbations are $\delta\rho/\rho = 3\delta T/T \leq 3 \times 10^{-5}$.[7] COBE's measurements had a resolution of $\sim 10°$, while BOOMERANG's and MAXIMA's were $\sim 0.2°$. These angular scales correspond to length scales of 2 Mpc and 50 kpc at the time of decoupling, and thus to 2 Gpc and 50 Mpc today. Thus we are only just beginning to detect void scale perturbations in the CMB. Although the magnitude of galaxy scale or even supercluster scale perturbations, are not yet directly constrained by observations, we will retain the figure of $\sim 10^{-5}$.

The scales associated with present day structures are summarised in the following table.

Table 1. Approximate scales associated with present day structures. The masses associated with the resolution scales of COBE, MAXIMA & BOOMERANG are obtained by assuming a density equal to the parabolic background value ρ_b, as indicated by '(1)' in the density coulmn. Useful collections of data can be found at `http://www.obspm.fr/messier/`, `http://adc.gsfc.nasa.gov/adc/sciencedata.html`, and `http://www.geocities.com/atlasoftheuniverse/supercls.html`.

	Radius today (kpc)	Mass ($M_\odot$)	Density of sphere (ρ_b)	Angle on CMB sky (°)
star	2×10^{-11}	1	2×10^{29}	8×10^{-7}
globular cluster	0.1	10^5	2×10^5	4×10^{-5}
galaxy	15	10^{11}	6×10^4	4×10^{-3}
Virgo cluster	2 000	2×10^{13}	5	0.02
Virgo supercluster	15 000	5×10^{14}	0.3	0.06
Abell cluster (example)	800	10^{15}	4 000	0.08
void	6×10^4	?		0.4
COBE resolution	1.6×10^6	1.9×10^{21}	(1)	10
BOOM/MAX resolution	3.1×10^4	1.5×10^{16}	(1)	0.2

We will use geometric units such that $c = 1 = G$, and the remaining scale freedom of GR is fixed by choosing the present day mass M_G of the condensation being considered as 1. The corresponding geometric length and time units are then:

$$L_G = M_G G/c^2 \quad , \qquad T_G = M_G G/c^3. \tag{5.5}$$

5.3 The Model

The principal limitation of the L-T model in the post-recombination era is the absence of rotation. However, once rotation has become a significant factor in the collapse process, there

is already a well defined structure. Later on pressure and viscosity will become important, but these factors only come into play once collapse is well underway. Because of the lack of rotation etc, all of which tend to delay or halt collapse, we expect our model to be rapidly collapsing rather than stationary at the present day.

We choose to model a cluster of galaxies chosen at random from the Abell catalogue:

$$M_{Abell\ Cluster} = 10^{15}\ M_{\odot}, \tag{5.6}$$

$$R_{Abell\ Cluster} = 800 \text{ kpc}. \tag{5.7}$$

From (5.5) and the above table the associated geometric units are

$$\begin{aligned} 1\ M_G &= M_{Abell\ Cluster}, \\ 1\ L_G &= 48 \text{ pc}, \\ 1\ T_G &= 156 \text{ years}, \\ \rightarrow \qquad R_{Abell\ Cluster} &= 16800\ L_G, \\ t_2 &= 6.4 \times 10^7\ T_G. \end{aligned} \tag{5.8}$$

At $t_2 = 10$ Gyrs $= 6.4 \times 10^7\ T_G$, we assume the final density profile to be

$$\rho_2(M) = \rho_{b,2}\left(7000\, e^{-(4M)^2}\right). \tag{5.9}$$

Now the Friedmann density at t_2 is:

$$\rho_{b,2} = 1.3 \times 10^{-17}\ M_G/L_G^3 \ = \ 8 \times 10^{-27}\ \text{kg/m}^3, \tag{5.10}$$

so the radius in the Friedmann 'background' that contains this mass is

$$R_{F,2} = \left(\frac{3M_{Abell\ Cluster}}{4\pi\rho_{b,2}}\right)^{1/3} \ = \ 260\,000\ L_G. \tag{5.11}$$

Thus we find

$$(R_2(M))^3 = \int_0^M \frac{3}{4\pi\rho_2(M')}\, dM' = \frac{3}{224\,000\sqrt{\pi}\ \rho_{b,2}} \text{erfi}(4M). \tag{5.12}$$

and the resulting $\rho_2(R)$ is shown in fig. 2.

At $t_1 = 100$ k years $= \ 10^{-5}\ t_2 \ = \ 641\ T_G$ we assume the initial density perturbation to have the density enhancement

$$3 \times 10^{-5} \rho_{b,1}, \tag{5.13}$$

for which the chosen profile is:

$$\rho_1(M) = \rho_{b,1}\left(\frac{1.00003\,(1 + 100\,M)}{1 + 100.003\,M}\right). \tag{5.14}$$

The Friedmann density at t_1 is:

$$\rho_{b,1} = 1.3 \times 10^{-7}\ M_G/L_G^3 \ = \ 8 \times 10^{-17}\ \text{kg/m}^3, \tag{5.15}$$

and the radius in the 'background' that contains the total mass is:

$$R_{F,1} = \left(\frac{3M_{Abell\ Cluster}}{4\pi\rho_{b,1}}\right)^{1/3} \ = \ 57\,000\ L_G. \tag{5.16}$$

The resulting $R_1(M)$ is

$$(R_1(M))^3 = \int_0^M \frac{3}{4\pi\rho_1(M')}\, dM' = \frac{3}{4\pi\rho_{b,1}}\left(M - \frac{0.00003}{100.003}\ln(1 + 100\,M)\right), \tag{5.17}$$

and the corresponding $\rho_1(R)$ is shown in fig. 2.

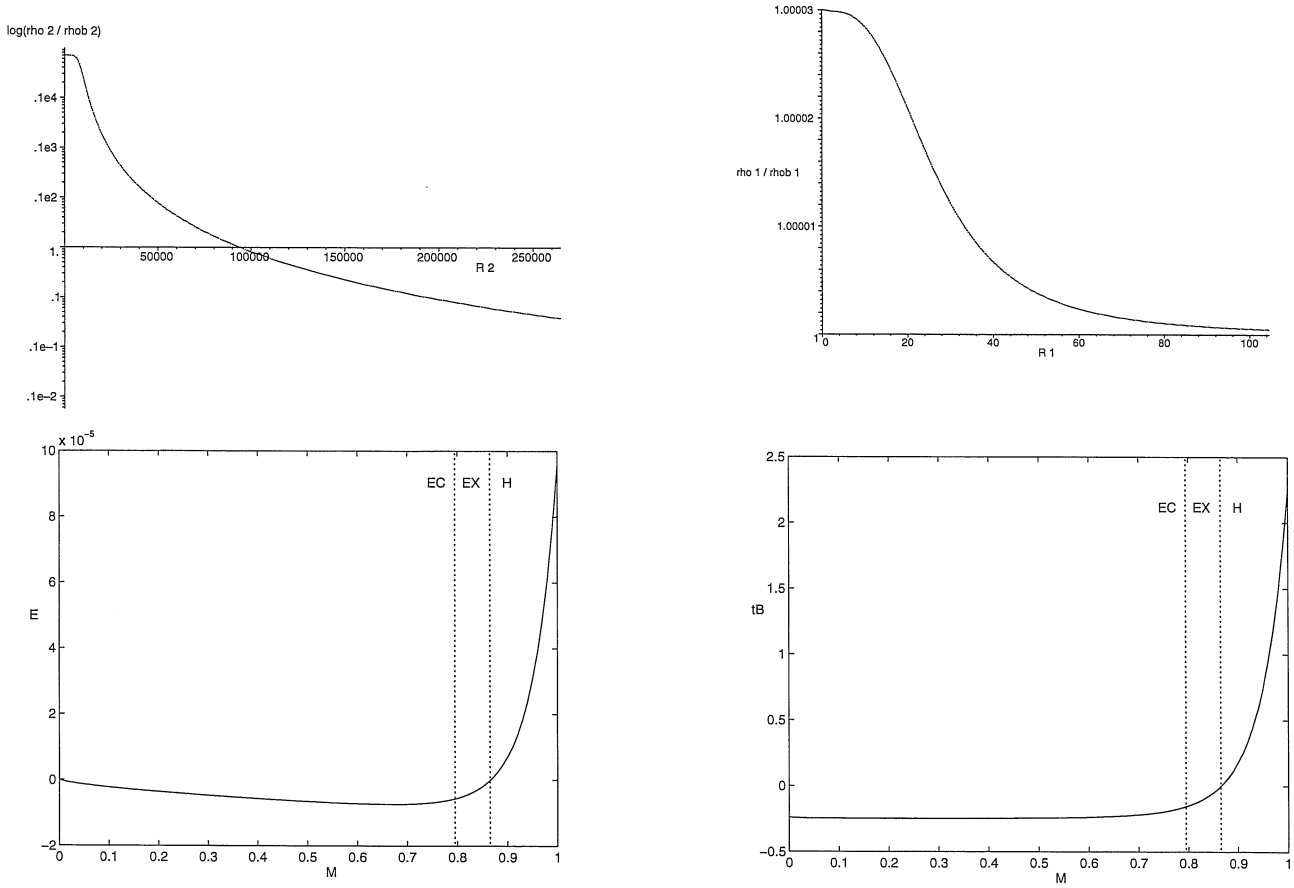

Figure 2. The density profile $\rho_2/\rho_{b,2}$ against areal radius R_2 (upper left); the density profile $\rho_1/\rho_{b,1}$ against areal radius R_1 (upper right); the L-T energy function $E(M)$ obtained from solving for the L-T model that evolves between $\rho_1(M)$ and $\rho_2(M)$ (lower left); and the L-T bang time function $t_B(M)$ obtained from solving for the L-T model that evolves between $\rho_1(M)$ and $\rho_2(M)$ (lower right). All axes are in geometric units. The symbols "EC", "EX" & "H" indicate regions that are respectively elliptic and recollapsing at t_2 (EC), elliptic and still expanding at t_2 (EX), and hyperbolic (H).

5.4 Model Results

A Maple program was written to generate the formulas and then solve for $E(M)$ and $t_B(M)$ numerically, as explained in sec. 3. The results are shown in figs. 2 and 3.

We see that E is of order 10^{-5} which gives a recollapse timescale of $10^7\ T_G = 1.7 \times 10^9$ yr, so that the curvature in the condensation is of order $Mt_2/(2E)^{3/2} \sim 0.17$. The bang time perturbation is of order $2\ T_G = 300$ years, and is quite negligible.

Strictly speaking, an increasing t_B creates a shell crossing, but for such a slight variation in t_B it occurs very early on, long before t_1 when the model becomes valid.

The 'velocity' $R_{,t}$ would, in a homogeneous model, increase as $M^{1/3}$, so plotting $R_{,t}/M^{1/3}$, as in fig. 3, indicates the velocity perturbation.

In this case, the perturbation is within 3.10^{-5} for $0 < M < 0.6$, where ρ_2 is large, but increases to 8.10^{-4} in the near vacuum region $0.6 < M < 1$. This slight excess is due to choosing a$\rho_2(M)$ that falls off outside the condensations, requiring a too strongly hyperbolic evolution that expands too rapidly. Still, this is within the limits allowed by CMB observations

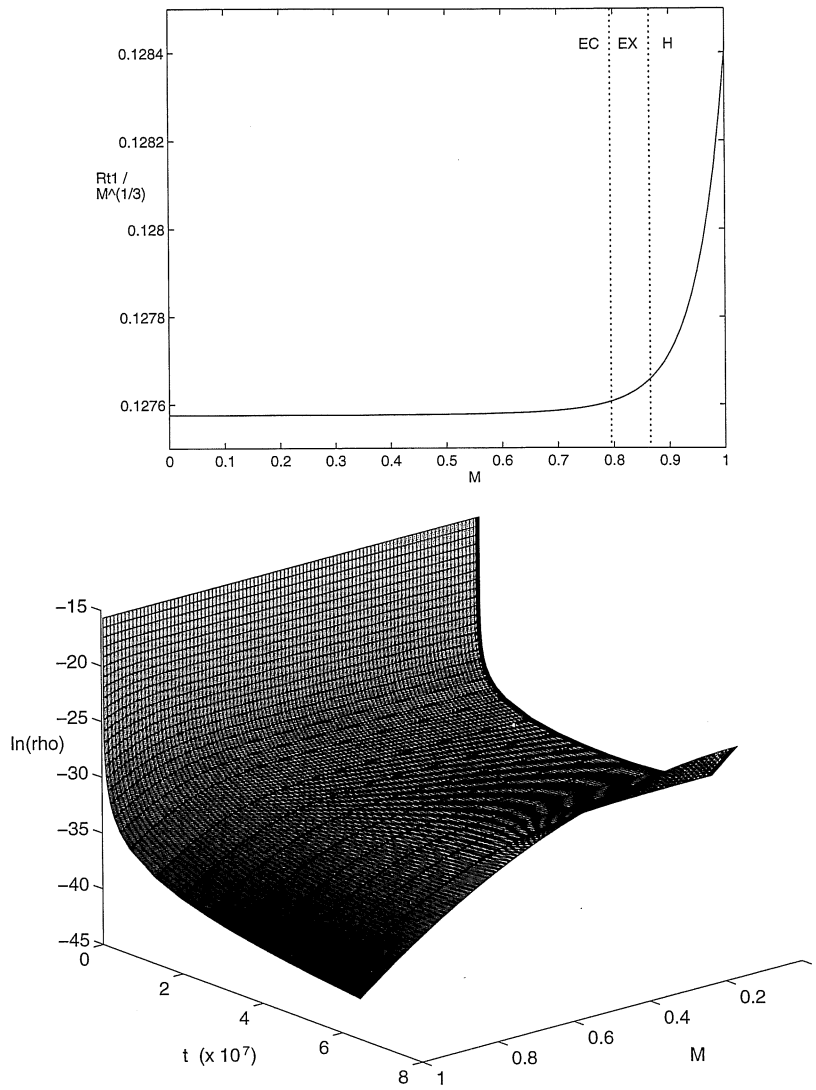

Figure 3. (a) The velocity perturbation $\dot{R}/M^{1/3}$ at time t_1 (top). A constant value would indicate no perturbation. (b) The evolution of $\rho(t, M)$ for the derived L-T model (bottom). All axes are in the geometric units of (5.5) & (5.8). In the range $0 < M < 0.795$ the evolution is elliptic and already recollapsing at time t_2, in $0.795 < M < 0.865$ it is elliptic but still expanding at t_2, and for $M > 0.865$ it is hyperbolic. In practice, recollapse would be halted at some point by the effects of pressure, rotation, etc. The initial and final density profiles calculated at times t_1 and t_2 coincide with those originally chosen and shown in fig. 2.

and their interpretation.[8]

As a cross-check, these derived functions were used in a separate MATLAB program that plots the evolution of a L-T model, given its arbitrary functions. The initial and final density profiles were recovered to high accuracy, see fig. 3.

6 Conclusions

We proved that an L-T model can evolve any initial density profile on a constant time slice, to any final density profile a given time later. Our numerical experiments show that realistic choices of the density profiles and the time difference generate reasonable models.

Our numerical example created an Abell cluster in a realistic timescale. It started from recombination, with a density perturbation $\delta\rho/\rho \sim 3.10^{-5}$. It then 'accreted' most of its

final mass. In fact this 'accretion' consists of lower expansion rates near the centre, and more rapid expansion further out. Only at late stages does actual collapse begin at the centre. The initial velocity perturbation turned out to be $\delta v/v \sim 3.10^{-5}$ within the future condensation and $\sim 8.10^{-4}$ in the future vacuum region, still within allowed limits.[8]

The theorem plus the numerical example demonstrate that the L-T model provides a very reasonable description of post-recombination structure formation.

These two points also indicate that post recombination structure formation in a dust universe has an important kinematical component — the initial distribution of velocities has as much bearing on whether or not a condensation forms, as the initial density distribution. These initial distributions of density and velocity are generated by the functions $E(M)$ and $t_B(M)$, i.e. coded in the initial conditions. It is the interplay between the initial density and initial velocity distributions that determines what structures are created. For example, as shown by Mustapha and Hellaby in an earlier paper,[9] there exists such a choice of initial conditions with which an initial condensation will evolve into a void.

At the time of writing this note, we have just completed further research into this topic.[10] We provided another example of a density to density evolution, with more realistic profiles at both t_1 and t_2. The profiles at t_2 were models of galaxy clusters and voids. We also showed that corresponding theorems and numerical schemes exist for the cases when either the initial state or the final state, or both, are specified by the velocity distribution $R_{,t}(M, t_i), i = 1, 2$. We provided more numerical examples in each case. These schemes should carry over to more general cosmological models, once they are found.

References

1. G. Lemaître, *Ann. Soc. Sci. Bruxelles* **A53**, 51 (1933); reprinted in *Gen. Rel. Grav.* **29**, 641 (1997).
2. R. C. Tolman, *Proc. Nat. Acad. Sci. USA* **20**, 169 (1934); reprinted in *Gen. Rel. Grav.* **29**, 935 (1997).
3. A. Krasiński, C. Hellaby, *Phys. Rev* D**65**, 023501 (2002).
4. A. Krasiński, "*Inhomogeneous Cosmological Models*", (Cambridge, U P, 1997).
5. C Hellaby, K. Lake, *Astrophys.* J. **290**, 381 (1985) [+ erratum: *Astrophys.* J. **300**, 461 (1985)].
6. W. B. Bonnor, *Phys. Lett.* A**112**, 26 (1985).
7. T. Padmanabhan "Cosmology and Astrophysics through problems", (Cambridge, U P, 1996).
8. P.K.S. Dunsby, *Class. Q. Grav.* **14**, 3391-3405 (1997).
9. N. Mustapha, C. Hellaby, *Gen. Rel. Grav.* **33**, 455 (2001).
10. A. Krasiński, C. Hellaby, *Phys. Rev.* D, submitted. See gr-qc 0303016.